Spatially-resolved Dense Molecular Gas Excitation in the Nearby LIRG VV 114

Toshiki Saito[1,2,3], Daisuke Iono[2,4], Daniel Espada[2,4], Kouichiro Nakanishi[2,4], Junko Ueda[2,5], Hajime Sugai[6], Min S. Yun[7], Shuro Takano[8], Masatoshi Imanishi[9], Tomonari Michiyama[2,4], Satoshi Ohashi[10], Minju Lee[1,2], Yoshiaki Hagiwara[11], Kentaro Motohara[12], Takuji Yamashita[13], Misaki Ando[2,4] and Ryohei Kawabe[1,2,4]

arXiv:1807.01325v1

ABSTRACT

We present high-resolution observations (0.″2–1.″5) of multiple dense gas tracers, HCN and HCO$^+$ (J = 1–0, 3–2, and 4–3), HNC (J = 1–0), and CS (J = 7–6) lines, toward the nearby luminous infrared galaxy VV 114 with the Atacama Large Millimeter/submillimeter Array. All lines are robustly detected at the central gaseous filamentary structure including the eastern nucleus and the Overlap region, the collision interface of the progenitors. We found that there is no correlation between star formation efficiency and dense gas fraction, indicating that the amount of dense gas does not simply control star formation in VV 114. We predict the presence of more turbulent and diffuse molecular gas clouds around the Overlap region compared to those at the nuclear region assuming a turbulence-regulated star formation model. The intracloud turbulence at the Overlap region might be excited by galaxy-merger-induced shocks, which also explains the enhancement of gas-phase CH_3OH abundance previously found there. We also present spatially resolved spectral line energy distributions of HCN and HCO$^+$ for the first time, and derive excitation parameters by assuming optically-thin and local thermodynamic equilibrium (LTE) conditions. The LTE model revealed that warmer, HCO$^+$-poorer molecular gas medium is dominated around the eastern nucleus, harboring an AGN. The HCN abundance is remarkably flat ($\sim 3.5 \times 10^{-9}$) independently of the various environments within the filament of VV 114 (i.e., AGN, star formation, and shock).

- 近傍LIRG VV114についてdense gas tracerの高空間分解能観測(0”.2-1”.5)
  - ➢ 輝線比画像
  - ➢ 星形成活動との関係
  - ➢ dense gasの物理状態

- VV114 (1”=420pc)
  - AGN (E0)
  - starburst region (E1)
  - shocked Overlap

- ALMAでの観測
  - HCN, HCO+
    - J=1-0, 3-2, 4-3
  - HNC J =1-0
  - CS J =7-6

- Σ_{SFR} : 110 GHz continuum
- HCN, HCO+のintegrated fluxとΣ_{SFR}の相関
- Jが大きくなると傾きが小さくなる
- ➢ 星形成が弱い(強い)ところで、励起能力が低い(高い)

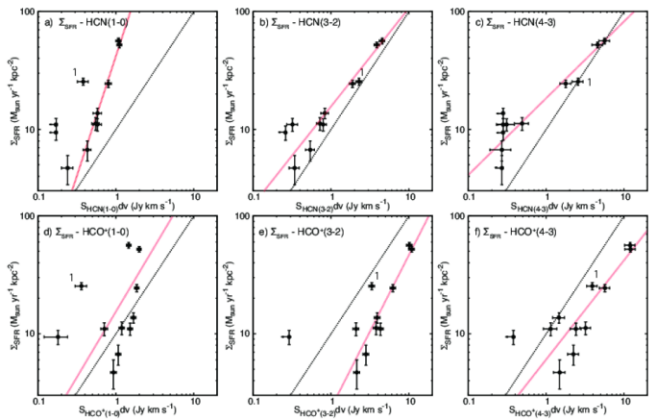

Figure 13. Plots of Σ_{SFR} against integrated fluxes of all HCN and HCO$^+$ transitions in log scale for the 3″apertures along the gaseous filament of VV 114 (see the inset of Figure 1b). These are the same as log L'_{dense}-log L_{IR} plots. The black dotted line corresponds to a line with a slope of unity. The data point corresponding to Region 1 is denoted as 1. The best fitted lines excluding Region 1 are shown as red dotted lines.

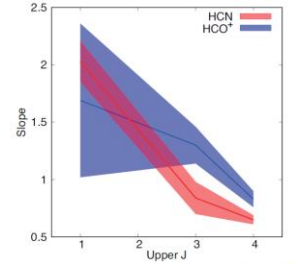

Figure 14. The index of the log-log plots shown in Figure 13. Red and blue tracks correspond to HCN and HCO$^+$ indices, respectively. 1σ error ranges of the fitting are shown as colorized areas.

- 各指標の分布
- ➢ E1付近で星形成活動はピーク
- ➢ f_{dense}の分布は異なる
- ➢ 星形成モデルとしてdensity threshold modelは合わない
  - $\Sigma_{SFR} \propto \Sigma_{dense} \propto f_{dense}\Sigma_{H2}$
- ➢ Merger induced shock

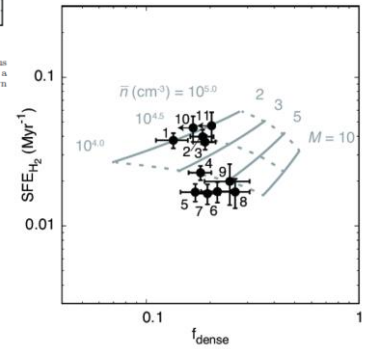

Figure 16. SFE_{H_2} plots against f_{dense}. Aperture IDs are shown for each data point. Grids of the turbulence-regulated star formation model are shown in grey curves (Krumholz & McKee 2005; Usero et al. 2015). Model curves with constant Mach number ($\mathcal{M}$) or constant average density ($\bar{n}$) are shown in solid or dashed curves, respectively.

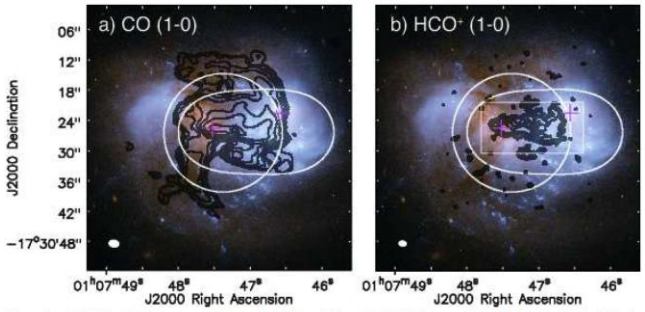

Figure 1. (a) ALMA CO (1–0) contours (Saito et al. 2015) overlaid on the HST/ACS image of VV 114 [Credit: NASA, ESA, the Hubble Heritage (STScI/AURA)-ESA/Hubble Collaboration, and A. Evans (University of Virginia, Charlottesville/NRAO/Stony Brook University)]. The contours are 0.2, 0.4, 0.8, 1.6, 3.2, 6.4, 12.8, 25.6, and 33.0 Jy beam^{-1} km s^{-1}. The white circle and ellipse show the field of view of Band 6 and Band 7, respectively. The magenta crosses show the positions of the nuclei defined by the peak positions of the 1.″0 resolution Ks-band image (Tateuchi et al. 2015). (b) Same as (a), but for HCO$^+$ (1–0). The contours are 0.67 × (0.04, 0.08, 0.16, 0.32, 0.64, and 0.96) Jy beam^{-1} km s^{-1}.

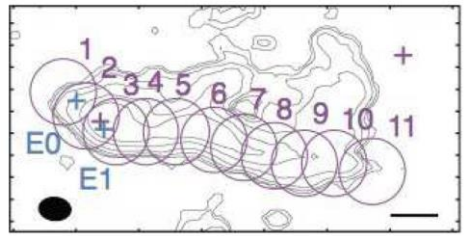

Figure 2. The central region of VV 114 as seen in HCO$^+$ (1–0) emission with the aperture and position names used for the flux measurements in this paper; E0 and E1 are the AGN and starburst (cyan crosses) as defined by Iono et al. (2013) and Region 1–11 are apertures along the central dust filament defined by Saito et al. (2017b). The magenta crosses show the positions of the nuclei defined by the peak positions of the 1.″0 resolution Ks-band image (Tateuchi et al. 2015). The scale bar corresponds to 2.″0 (= 840 pc).

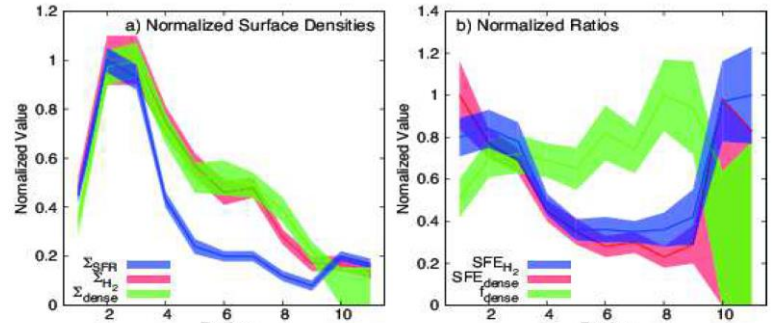

Figure 15. (a) Normalized distributions of Σ_{SFR} (blue), Σ_{H_2} (red), and Σ_{dense} (green) along the filament of VV 114. The absolute values are found in Table 4 and Table 2 of Saito et al. (2017a). (b) Normalized distributions of SFE_{H_2} (blue), SFE_{dense} (red), and f_{dense} (green) along the filament of VV 114. The absolute values are found in Table 4. We note that the Overlap region shows higher f_{dense}, but lower SFE_{H_2} and SFE_{dense} (see text in detail).